

Neural variance reduction for stochastic differential equations

P.D. Hinds * M.V. Tretyakov[†]

September 27, 2022

Abstract

Variance reduction techniques are of crucial importance for the efficiency of Monte Carlo simulations in finance applications. We propose the use of neural SDEs, with control variates parameterized by neural networks, in order to learn approximately optimal control variates and hence reduce variance as trajectories of the SDEs are being simulated. We consider SDEs driven by Brownian motion and, more generally, by Lévy processes including those with infinite activity. For the latter case, we prove optimality conditions for the variance reduction. Several numerical examples from option pricing are presented.

Keywords: stochastic differential equations, control variates, deep learning, option pricing.

1 Introduction

Stochastic differential equations (SDEs) driven by Lévy processes arise as a modelling tool in several fields including finance, insurance, physics, and chemistry ([7, 29, 25]). In finance (see e.g. [6, 7, 19, 43] and references therein) SDEs are used for pricing and hedging financial derivatives with the aims to find current prices and hedges of options which are not traded or not regularly traded on exchanges and to evaluate future option prices for risk management purposes.

In many cases including option pricing, one wants to compute the value

$$u(t, x) = \mathbb{E} \left[f(X_{t,x}(T)) \right], \quad (1.1)$$

where $X_{t,x}(s)$, $s \geq t$, is the solution to a system of SDEs with the initial condition $X_{t,x}(t) = x$, $T > 0$ is a terminal (maturity) time, and f is a real-valued function (payoff in the case of option pricing). Weak-sense numerical integration of SDEs together with the Monte Carlo (MC) technique can be used to find $u(t, x)$ [19, 34, 37]. When employing these probabilistic methods, there are two sources of the error present in the numerical approximations: the numerical integration error and the MC error. Methods of variance reduction play an important role in minimizing the MC error which is the focus of this paper.

As it is well known (see e.g. [12, 13]), the function $u(t, x)$ solves the related, via the Feynman-Kac formula, partial differential equation (PDE) problem in the diffusion case or partial integro-differential equation (PIDE) problem in the case of general Lévy processes driven SDEs. When SDEs are driven purely by Brownian motion, there is an optimality condition (see [36, 31, 34] or Theorem 1 here) relating the optimal variance reduction with the solution of the PDE problem, $u(t, x)$, and its spatial derivatives, $\partial u(t, x)/\partial x^i$. Of course, if the PDE solution $u(t, x)$

*School of Mathematical Sciences, University of Nottingham, UK; pmxph7@nottingham.ac.uk

[†]School of Mathematical Sciences, University of Nottingham, UK; Michael.Tretyakov@nottingham.ac.uk

is known, there would be no need to resort to probabilistic methods in the first place. The importance of this theoretical result lies in the fact that it demonstrates that perfect variance reduction is possible and, if an approximation of the solution $u(t, x)$ can be learned, it can induce efficient variance reduction. In addition, this variance reduction method does not bias the MC approximation (see e.g. [36, 33, 34]), indicating that the approximation of the required $u(t, x)$ and its derivatives need not have a high accuracy in order to be useful.

To make variance reduction practical, a suitable method of constructing $u(t, x)$ and its spatial derivatives should be inexpensive. Hence, a trade-off between accuracy and computational costs in finding $u(t, x)$ and $\partial u(t, x)/\partial x^i$ is needed. To address this problem, it was suggested in [33] (see also [34] and [4]) to exploit conditional probabilistic representations of $u(t, x)$ in conjunction with linear regression, which allows us to evaluate $u(t, x)$ and $\partial u(t, x)/\partial x^i$ using the single auxiliary set of approximate trajectories starting from an initial position. This leads to obtaining sufficiently inexpensive, but useful for variance reduction, estimates of $u(t, x)$ and $\partial u(t, x)/\partial x^i$. The drawback of this approach is reliance on linear regression. To make it computationally feasible, a careful selection of basis functions for linear regression is needed. This selection is heavily problem dependent and limits applicability of this variance reduction approach.

In this direction, Vidales, Šiška and Szpruch [45] propose several algorithms with the aim of constructing a control variate via deep learning. An analogue of the linear regression algorithm from [33] is proposed, this time using a deep neural network to approximate the PDE solution. Again, the rough solution will be biased, but the bias is removed from the actual approximation by using the MC technique. In addition to this, a method is put forward to learn the control variates directly, without first constructing a solution to the PDE. In order to do this, the empirical variance is used as a loss function and minimized using stochastic gradient descent. In all cases, the training of neural networks is carried out offline over a parametric family of SDEs (PDEs). In the context of financial option pricing, this means that training one network is sufficient for a single model-payoff combination.

The key objective of our paper is to show that deep learning (i.e. nonlinear regression) can successfully replace linear regression in variance reduction for SDEs in a universal manner, i.e. without need to do tuning for each new system of SDEs which is important for applications, in particular for those arising in financial engineering. The use of neural networks instead of linear regression as in [33] eliminates the need of finding a specific set of basis functions, thus making the variance reduction truly practical.

Furthermore, in contrast to [45] and many other deep learning works related to computational finance and more generally to efficient SDEs and PDEs simulations (see e.g. [40, 21, 16, 41] and references therein), here we do not rely on an (often costly) offline training of neural networks but rather we do network training online together with actual simulation of the required expectation $u(t, x)$ with reduced variance. In other words, we propose a black-box fashion practical variance reduction tool which does not require any lengthy pre-training and tuning, analogously how the variance reduction method of [33] intended to work but without the limitations due to linear regression.

For general Lévy-driven SDEs, variance reduction has been considerably less studied than in the Brownian case. To the best of our knowledge, a result demonstrating that there exists an optimal choice of control variates, analogous to the results (in the diffusion case) in [36, 31] (see also [34]), does not exist. We note that in the context of financial applications, there have been several effective approaches towards variance reduction under Lévy-driven models (e.g. [39, 11, 38] and references therein).

We also remark that there are other techniques than variance reduction aimed at reducing computational complexity of MC simulations: multi-level MC method [17] and quasi-Monte Carlo method [10]. They have their own areas of applicability and can potentially be combined with deep learning and neural SDEs considered in this paper. Here, we restrict ourselves with considering the use of deep learning for improving the plain-vanilla MC technique via variance reduction.

This paper is most closely related to [31, 33, 45]. We show that for Lévy-driven SDEs, there exist conditions ensuring the optimal variance reduction, which is an analogous result to the one in the Brownian SDEs case [31]. We also provide details of a novel algorithm which produces low variance simulations of a given SDEs system. Given a system of SDEs, we introduce control variates and parameterize them with neural networks. This can be interpreted in two ways. First, we can treat the problem of fitting the neural network as a nonlinear regression problem, for which we need to solve an optimization problem. As such, the proposed method can be seen as a more general framework than that proposed in [33]. Second, the use of a neural network as a coefficient in SDEs gives rise to neural SDEs (see e.g. [44, 23]), which is essentially a generative model (see [26]). Regardless of the perspective, the parameters of the neural SDEs can be learned from numerical simulations of the system, in such a way that the empirical variance is minimized. SDEs' trajectories with high accuracy can then be simulated using the approximate control variates. We leverage the fact that no prescribed accuracy is required for approximated control variates, since they do not introduce bias into the MC approximation. This algorithm is not limited to the case that SDEs are driven only by Brownian motion, as in [33, 45], and can be applied in the general setting of Lévy noise, even when we have infinite activity of jumps.

The paper is structured as follows. In Section 2, we consider the case where SDEs are driven purely by Brownian motion and the corresponding PDE problem. We recall the optimality conditions for variance reduction and present a numerical algorithm to find an approximation of the optimal control variate using deep learning. In Section 3, we consider the more general case where SDEs are driven by Lévy noise. We derive optimality conditions for variance reduction and present a corresponding numerical algorithm. Section 4 contains several numerical examples of computing option prices with SDEs models of underliers in both the Brownian motion and Lévy noise cases. In the Lévy noise case, especially for SDEs driven by infinite activity Lévy processes, efficient approximation of the SDEs requires the use of jump-adapted numerical schemes (see e.g. [9] and references therein) which pose a unique challenge (addressed in Section 4) of how to simulate independent trajectories in parallel since each trajectory may have a different number of time steps. By our numerical tests, we show that the proposed neural variance reduction technique can considerably reduce variance and hence increase computational efficiency (up to 40 times) of option pricing.

2 SDEs driven by Brownian motion

In the case of SDEs driven only by Brownian motion, the two variance reduction methods of importance sampling and control variates are well-known and have been studied in [36, 31, 34] and references therein.

Let $(\Omega, \mathcal{F}, \{\mathcal{F}_t\}_{t_0 \leq t \leq T}, P)$ be a filtered probability space on which a d -dimensional Brownian motion $W(t)$ is defined. For $s \in [t_0, T]$ and $x \in \mathbb{R}^d$, consider the stochastic processes $X_{s,x}(t), Y_{s,x}(t), Z_{s,x}(t), t \geq s$, defined as the solution to the system:

$$dX(t) = b(t, X)dt + \sigma(t, X)dW(t), \quad X(s) = x, \quad (2.1)$$

$$dY(t) = c(t, X)Y(t)dt, \quad Y(s) = 1, \quad (2.2)$$

$$dZ(t) = g(t, X)Y(t)dt, \quad Z(s) = 0, \quad (2.3)$$

where $b(t, x)$ is a d -dimensional vector, $\sigma(t, x)$ is a $d \times d$ matrix, and $c(t, x)$ and $g(t, x)$ are scalar functions, all with appropriate regularity properties [13, 14]. We are interested in calculating the quantity

$$u(s, x) = \mathbb{E}[f(X_{s,x}(T))Y_{s,x}(T) + Z_{s,x}(T)]. \quad (2.4)$$

Let us denote the random variable of interest as

$$\Gamma := \Gamma_{s,x} := f(X_{s,x}(T))Y_{s,x}(T) + Z_{s,x}(T), \quad (2.5)$$

and, more generally, let us define

$$\Gamma(t) := \Gamma_{s,x}(t) := u(t, X_{s,x}(t))Y_{s,x}(t) + Z_{s,x}(t), \quad (2.6)$$

noting that $\Gamma_{s,x}(T) = \Gamma_{s,x}$. The function $u : [t_0, T] \times \mathbb{R}^d \rightarrow \mathbb{R}$ is known [12, 13, 14] to satisfy the related Cauchy problem for the parabolic PDE:

$$\frac{\partial u}{\partial t} + Lu + c(t, x)u + g(t, x) = 0, \quad (t, x) \in [t_0, T] \times \mathbb{R}^d \quad (2.7)$$

$$u(T, x) = f(x), \quad x \in \mathbb{R}^d, \quad (2.8)$$

where L is a differential operator of the form

$$Lu(t, x) := \frac{1}{2} \text{tr}[a(t, x)\nabla^2 u(t, x)] + \langle b(t, x), \nabla u(t, x) \rangle. \quad (2.9)$$

Here $a(t, x) = \sigma(t, x)\sigma^\top(t, x)$ is a symmetric positive semi-definite $d \times d$ -matrix.

Instead of the system (2.1)-(2.3), consider now the system

$$dX = b(t, X)dt - \sigma(t, X)\mu(t, X)dt + \sigma(t, X)dW(t), \quad X(s) = x, \quad (2.10)$$

$$dY = c(t, X)Ydt + \mu^\top(t, X)YdW(t), \quad Y(s) = 1, \quad (2.11)$$

$$dZ = g(t, X)Ydt + G^\top(t, X)YdW(t), \quad Z(s) = 0, \quad (2.12)$$

where μ and G are d -dimensional vector functions with good analytical properties. Note that the system (2.1)-(2.3) is a special case of this system with $\mu = G = 0$. It is straightforward to show that while $\mathbb{E}\Gamma(T)$ does not depend on μ or G , the variance of $\Gamma(T)$ does indeed depend on them (see e.g. [34]). The case when $\mu = 0$ corresponds to the method of control variates (first considered in [36, 35]). The case when $G = 0$ corresponds to the method of importance sampling (first considered in [18, 46]). The combining method, i.e. using both importance sampling and control variates simultaneously, was introduced in [31] (see also [34]). Those methods can be made optimal, in the sense that $\Gamma(T)$ becomes deterministic through an optimal choice of μ or/and G . This optimal choice (see the theorem below), however, depends on (and consequently requires knowledge of) the full solution of the related PDE problem and its spatial derivatives.

Theorem 1 (Milstein & Schoenmakers). *If μ and G are such that*

$$u(t, x)\mu(t, x) + G(t, x) = -\sigma^\top(t, x)\nabla u(t, x) \quad (2.13)$$

for all $(t, x) \in [s, T] \times \mathbb{R}^d$, then $\text{Var}\Gamma_{s,x}(T) = 0$.

This theorem demonstrates a general possibility of perfect variance reduction and serves as a guidance towards choosing (some suboptimal but practical) μ or/and G .

2.1 Numerical algorithm

We consider the neural SDEs

$$dX = b(t, X)dt + \sigma(t, X)dW(t), \quad X(s) = x, \quad (2.14)$$

$$dY = c(t, X)Ydt, \quad Y(s) = 1, \quad (2.15)$$

$$dZ = g(t, X)Ydt + G_\theta^\top(t, X)YdW(t), \quad Z(s) = 0, \quad (2.16)$$

where $G_\theta : [t_0, T] \times \mathbb{R}^d \rightarrow \mathbb{R}^d$ is a neural network parameterization of G (see Appendix A).

Provided that the system (2.1)-(2.3) has a unique solution, it is sufficient that G_θ be Lipschitz in x for the existence and uniqueness of a solution to (2.14)-(2.16). In the case of feed-forward

architectures, which we will make use of, this amounts to G_θ having a Lipschitz activation function (see Appendix A).

Comparably to before, define

$$\Gamma_\theta := f(X_{s,x}(T))Y_{s,x}(T) + Z_{s,x}(T). \quad (2.17)$$

The subscript θ in Γ_θ denotes the implicit dependence of Γ_θ on G_θ .

For any choice of θ , the expectation, $\mathbb{E}\Gamma_\theta$, remains unchanged. Moreover, since Theorem 1 implies that there exists an optimal choice of G such that we have zero variance of Γ , our objective is to find parameters θ^* such that G_{θ^*} approximately satisfies (2.13) and hence $\text{Var}\Gamma_{\theta^*} \approx 0$. We will denote the true optimal value of G by G^* . In other words, G^* satisfies

$$G^*(t, x) = -\sigma^\top(t, x)\nabla u(t, x). \quad (2.18)$$

Let us briefly justify the choice of feed-forward neural networks as approximators. There exists many theoretical results on the expressivity of neural networks [8, 24, 3]. In particular, the universal approximation theorem given by Hornik et al. [24] states that for any finite measure on $(\mathbb{R}, \mathcal{B}(\mathbb{R}))$, the class of feed-forward neural networks, mapping from \mathbb{R}^d to \mathbb{R} with continuous and non-constant activation is dense in L^p . The function we would like to approximate, G^* , maps into \mathbb{R}^d but the above approximation theorem can be applied componentwise.

The problem of finding optimal parameters θ^* amounts to solving the optimization problem

$$\theta^* \in \arg \min_\theta \text{Var}\Gamma_\theta. \quad (2.19)$$

Of course, in any non-trivial situation $\text{Var}\Gamma_\theta$ can not be evaluated analytically, nor can the random variable Γ_θ be simulated exactly. Instead we must use the empirical (sample) variance of independent realizations of an approximate random variable, $\bar{\Gamma}_\theta$, which is close to Γ_θ in the weak sense. Fixing a large $M_r \in \mathbb{N}$, the problem becomes

$$\theta^* \in \arg \min_\theta \text{Var}_{M_r}\bar{\Gamma}_\theta, \quad (2.20)$$

where $\text{Var}_{M_r}(\cdot)$ denotes the empirical variance over M_r realizations. The random variables $(\bar{\Gamma}_{\theta,m})_{m=1}^{M_r}$ are obtained by numerical integration of the neural SDE system (2.14)-(2.16) together with (2.17). This optimization problem can be solved using stochastic gradient descent (SGD), noting that the loss function

$$\mathcal{L}(\theta) := \text{Var}_{M_r}\bar{\Gamma}_\theta \quad (2.21)$$

is differentiable.

Once the parameters θ^* have been found, realizations of $\bar{\Gamma}_{\theta^*}$ can be simulated using a (potentially different) numerical integration scheme. The new MC estimator is then given by

$$\bar{u}(s, x) = M^{-1} \sum_{m=1}^M \bar{\Gamma}_{\theta^*,m}, \quad (2.22)$$

where $(\bar{\Gamma}_{\theta^*,m})_{m=1}^M$ are independent copies of $\bar{\Gamma}_{\theta^*}$.

This motivates a two-pass algorithm, where the first pass finds optimal parameters θ^* and the second pass uses these parameters to simulate low-variance random variables for the MC estimator (cf. the two-run algorithm in [33]). This is described in Algorithm 1. In the first pass, we simulate (using a numerical integration scheme) trajectories of the solution to the system (2.14)-(2.16) with $G_\theta = 0$ and store them in memory along with the random variables used in the scheme. These trajectories can then be used to simulate the θ -dependent term, $\int_s^T G_\theta(t, X)Y(t)dW(t)$, at each iteration of the SGD algorithm. This eliminates the need to simulate the entire system for each iteration of SGD.

In the second pass, we simply simulate solutions to the system (2.14)-(2.16) using G_{θ^*} . Note that the numerical scheme used in the second pass does not need to have anything in common with the numerical scheme of the first pass. In particular, we find it to be effective to use a coarse grid (larger h) in the first pass, followed by a fine grid (smaller h) in the second pass (cf. a similar observation in [33] in the case of the linear regression-based algorithm).

Letting $V(t) = (X(t)^\top, Y(t), Z(t)^\top)^\top$ and $v = (x^\top, 1, 0)^\top$, we consider numerical methods with a uniform step-size $h > 0$ of the form:

$$\bar{V}_{k+1} = \bar{V}_k + A(t_k, \bar{V}_k, h, \xi_k), \quad (2.23)$$

$$\bar{V}_0 = V(s) = v, \quad (2.24)$$

for some Borel measurable, vector-valued function A and random variables $(\xi_n)_{n \geq 0}$, where ξ_0 is independent of \bar{V}_0 and ξ_k is independent of $(\xi_n)_{0 \leq n < k}$ and $(\bar{V}_n)_{0 \leq n \leq k}$. We denote the scheme by (A, h) .

Algorithm 1: Neural control variate method for Brownian-driven SDEs

Result: MC approximation of the solution to the PDE (2.7)-(2.8), $\bar{u}(s, x_0)$

Initialise: Number of trials for first-pass M_r , number for trials for second-pass M , numerical scheme for first-pass (A_r, h_r) , numerical scheme for second-pass (A, h)

for $m \leftarrow 1$ **to** M_r **do**

Initialise: $\bar{X}_0, \bar{Y}_0, \bar{Z}_0 \leftarrow x_0, 1, 0$

Compute: $(t_k, \bar{X}_k, \bar{Y}_k, \bar{Z}_k)_{0 < k < N}^m$ and $(\bar{\Gamma})^m$ according to (2.14)-(2.16) with $G_\theta = 0$ and the scheme (A_r, h_r)

Store: $(t_k, \bar{X}_k, \bar{Y}_k, \bar{Z}_k)_{0 < k < N}^m$ and $(\bar{\Gamma})^m$ and random variables $(\xi_k)_{0 \leq k < N}$

end

Compute: $\theta^* = \arg \min_{\theta \in \Theta} \text{Var}_{M_r} \bar{\Gamma}_\theta$ by SGD using the stored trajectories and random variables to compute $\bar{\Gamma}_\theta$ with the scheme (A_r, h_r) .

for $m \leftarrow 1$ **to** M **do**

Initialise: $\bar{X}_0, \bar{Y}_0, \bar{Z}_0 \leftarrow x_0, 1, 0$

Compute: $\bar{\Gamma}_{\theta^*, m}$ using (2.14)-(2.16) with G_{θ^*} and the numerical scheme (A, h)

Store: Updated sample statistics of $\bar{\Gamma}_{\theta^*}$

end

Return: $\bar{u}(s, x_0) = M^{-1} \sum_{m=1}^M \bar{\Gamma}_{\theta^*, m}$

Remark 1. During the training phase of Algorithm 1 (i.e. the first-pass), we proposed to first simulate all trajectories of the system of SDEs and then perform SGD while these trajectories are stored in memory. Alternatively, the simulation can be performed alongside SGD. In other words, a single batch of trajectories can be simulated followed by one step of SGD. While the demands on memory are lessened, more unique trajectories have to be simulated.

In practice the learned G_{θ^*} is not equal to the optimal G^* satisfying (2.18) due to errors of deep learning (finite size of the network, limited training set and accuracy of SGD) and due to the numerical integration error. Recall [34, p. 151]:

$$\text{Var} \Gamma_{\theta^*} = E \int_s^T Y_{s, x_0}^2(t) \sum_{j=1}^d \left(\sum_{i=1}^d \sigma^{ij} \frac{\partial u}{\partial x^i} + G_{\theta^*}^j \right)^2 dt.$$

Then, using (2.18), we get that the standard deviation of Γ_{θ^*} gives the error of Γ_{θ^*} in a weighted norm:

$$\sqrt{\text{Var} \Gamma_{\theta^*}} = \left(E \int_s^T Y_{s, x_0}^2(t) |G_{\theta^*} - G^*|^2 dt \right)^{1/2}.$$

Consequently, ignoring the error of numerical integration, we can view

$$\text{Err}_{G_{\theta^*}} = \frac{\sqrt{\text{Var}\Gamma_{\theta^*}}}{\mathbb{E}\Gamma_{\theta^*}} \quad (2.25)$$

as the appropriated relative error of the trained G_{θ^*} .

3 SDEs driven by Lévy processes

We now turn our attention to the case of SDEs driven by a more general Lévy noise, i.e., SDEs driven by both Wiener and Poisson processes. In this case, we have the corresponding Cauchy problem for the PIDE:

$$\frac{\partial u}{\partial t} + Lu + c(t, x)u + g(t, x) = 0, \quad (t, x) \in [t_0, T] \times \mathbb{R}^d, \quad (3.1)$$

$$u(T, x) = f(x), \quad x \in \mathbb{R}^d, \quad (3.2)$$

where L is a partial integro-differential operator of the form

$$\begin{aligned} Lu(t, x) := & \frac{1}{2} \text{tr}[a(t, x)\nabla^2 u(t, x)] + \langle b(t, x), \nabla u(t, x) \rangle \\ & + \int_{\mathbb{R}^q} \left[u(t, x + F(t, x)z) - u(t, x) - \langle F(t, x)z, \nabla u(t, x) \rangle \mathbb{1}_{|z| \leq 1} \right] \nu(dz). \end{aligned} \quad (3.3)$$

Here $a(t, x)$ is a symmetric positive semidefinite $d \times d$ -matrix, $b(t, x)$ is a d -dimensional vector, $c(t, x)$ and $g(t, x)$ are scalar functions, $F(t, x)$ is a $d \times q$ -matrix, and ν is a Lévy measure such that $\int_{\mathbb{R}^q} (|z|^2 \wedge 1) \nu(dz) < \infty$. We allow for the possibility that ν is of infinite intensity, i.e. we may have $\nu(B(0, r)) = \infty$ for some $r > 0$, where as usual for $x \in \mathbb{R}^d$ and $r > 0$ we write $B(x, r)$ for the open ball of radius r centred at x . Conditions for the existence and uniqueness of a solution to the problem (3.1)-(3.2) can be found in [15].

Let $(\Omega, \mathcal{F}, \{\mathcal{F}_t\}_{t_0 \leq t \leq T}, P)$ be a filtered probability space on which a d -dimensional standard Wiener process $w(t)$ and a Poisson random measure N on $[0, \infty) \times \mathbb{R}^q$ with intensity $ds \times \nu(dz)$ are defined. Let \hat{N} denote the corresponding Poisson random measure with compensated small jumps. That is, for all $B \in \mathcal{B}(R^q)$, $t \geq 0$,

$$\hat{N}([0, t] \times B) = \int_{[0, t] \times B} (N(ds, dz) - \mathbb{1}_{|z| \leq 1} \nu(dz) ds). \quad (3.4)$$

We assume that the problem (3.1)-(3.2) admits a classical solution, $u \in C^{1,2}([t_0, T] \times \mathbb{R}^d)$. It has the probabilistic representation (see e.g. [1, 7]) given by

$$u(s, x) = \mathbb{E}[f(X_{s,x}(T))Y_{s,x}(T) + Z_{s,x}(T)], \quad (3.5)$$

where $X_{s,x}(t)$, $Y_{s,x}(t)$, $Z_{s,x}(t)$, $s \leq t \leq T$, is the solution of the system of SDEs:

$$dX = b(t, X)dt + \sigma(t, X)dw(t) + \int_{\mathbb{R}^q} F(t, X(t-))z\hat{N}(dt, dz), \quad X(s) = x, \quad (3.6)$$

$$dY = c(t, X)Y(t-)dt, \quad Y(s) = 1, \quad (3.7)$$

$$dZ = g(t, X)Y(t-)dt, \quad Z(s) = 0. \quad (3.8)$$

Here the matrix $\sigma(t, x)$ is a solution of the equation $a(t, x) = \sigma(t, x)\sigma^\top(t, x)$.

In order to be able to efficiently simulate approximate realisations of the process X , we follow [2] (see also [28, 9]) and consider a modified process X^ε , where the small jumps of X

are approximated with an additional diffusion component. The resulting X^ε is a jump-diffusion with only finitely many jumps on any finite time interval.

Let $W(t)$ be a q -dimensional Brownian motion independent of w and N . Then the process $X_{s,x}^\varepsilon(t)$ and the corresponding $Y_{s,x}^\varepsilon(t)$, $Z_{s,x}^\varepsilon(t)$ are defined as the solution to

$$\begin{aligned} dX^\varepsilon &= b(t, X^\varepsilon(t-)) - F(t, X^\varepsilon(t-))\gamma_\varepsilon dt + \sigma(t, X^\varepsilon(t-))dw(t) \\ &\quad + F(t, X^\varepsilon(t-))\beta_\varepsilon dW(t) + \int_{|z|\geq\varepsilon} F(t, X^\varepsilon(t-))zN(dt, dz), \end{aligned} \quad (3.9)$$

$$dY^\varepsilon = c(t, X^\varepsilon)Y^\varepsilon(t-)dt, \quad (3.10)$$

$$dZ^\varepsilon = g(t, X^\varepsilon)Y^\varepsilon(t-)dt, \quad (3.11)$$

with the same initial conditions as in (3.6)-(3.8). The vector γ_ε is defined component-wise as

$$\gamma_\varepsilon^i = \int_{\varepsilon \leq |z| \leq 1} z^i \nu(dz), \quad (3.12)$$

and β_ε is defined by

$$B_\varepsilon^{ij} = \int_{|z|<\varepsilon} z^i z^j \nu(dz), \quad \beta_\varepsilon \beta_\varepsilon^\top = B_\varepsilon. \quad (3.13)$$

As before, introduce the random variable of interest as

$$\Gamma^\varepsilon := \Gamma_{s,x}^\varepsilon := f(X_{s,x}(T))Y_{s,x}^\varepsilon(T) + Z_{s,x}^\varepsilon(T), \quad (3.14)$$

and, more generally,

$$\Gamma^\varepsilon(t) := \Gamma_{s,x}^\varepsilon(t) := u(t, X_{s,x}^\varepsilon(t))Y_{s,x}^\varepsilon(t) + Z_{s,x}^\varepsilon(t), \quad (3.15)$$

noting that $\Gamma^\varepsilon = \Gamma^\varepsilon(T)$.

We can approximate the solution, $u(t, x)$, to the PIDE (3.1)-(3.2) by

$$u(s, x) \approx u^\varepsilon(s, x) := \mathbb{E}[\Gamma^\varepsilon(T)]. \quad (3.16)$$

It is shown in [9] (see also [28]) that $u^\varepsilon(t, x)$ is a good approximation for $u(t, x)$, whose accuracy is controlled by ε . The PIDE problem for u^ε is given by

$$\frac{\partial u}{\partial t} + L_\varepsilon u^\varepsilon + c(t, x)u^\varepsilon + g(t, x) = 0, \quad (3.17)$$

$$u^\varepsilon(T, x) = f(x), \quad (3.18)$$

where L_ε is the partial integro-differential operator

$$\begin{aligned} L_\varepsilon v(t, x) &:= \frac{1}{2} \text{tr} \left[(a(t, x) + F(t, x)B_\varepsilon F^\top(t, x)) \nabla^2 v(t, x) \right] + \langle b(t, x) - F(t, x)\gamma_\varepsilon, \nabla v(t, x) \rangle \\ &\quad + \int_{|z|\geq\varepsilon} [v(t, x + F(t, x)z) - v(t, x)] \nu(dz). \end{aligned} \quad (3.19)$$

In the same spirit as in the Brownian case considered in Section 2, we modify the system (3.9)-(3.11) to allow for variance reduction of Γ^ε without changing the expectation of Γ^ε . In this case we have three sources of noise, namely w , W , and N . For the Brownian motions, we use importance sampling and control variate analogously to the results of Section 2. In addition, we need a control variate to deal with the Poisson random measure N . To this end, we introduce the five auxiliary functions, $\mu_w : [0, \infty) \times \mathbb{R}^d \rightarrow \mathbb{R}^d$, $\mu_W : [0, \infty) \times \mathbb{R}^d \rightarrow \mathbb{R}^q$, $G_w : [0, \infty) \times \mathbb{R}^d \rightarrow \mathbb{R}^d$,

$G_W : [0, \infty) \times \mathbb{R}^d \rightarrow \mathbb{R}^q$, and $G_N : [0, \infty) \times \mathbb{R}^{d+q} \rightarrow \mathbb{R}$, which can be arbitrary except for some regularity conditions.

Consider now the system

$$dX^\varepsilon = \left[b(t, X^\varepsilon(t-)) - F(t, X^\varepsilon(t-))\gamma_\varepsilon - \sigma(t, X^\varepsilon(t-))\mu_w(t, X^\varepsilon(t-)) - F(t, X^\varepsilon(t-))\beta_\varepsilon\mu_W(t, X^\varepsilon(t-)) \right] dt \quad (3.20)$$

$$+ \sigma(t, X^\varepsilon(t-))dw(t) + F(t, X^\varepsilon(t-))\beta_\varepsilon dW(t) + \int_{|z| \geq \varepsilon} F(t, X^\varepsilon(t-))zN(dt, dz),$$

$$dY^\varepsilon = c(t, X^\varepsilon(t-))Y(t-)dt + Y(t-)\mu_w^\top(t, X^\varepsilon(t-))dw(t) + Y(t-)\mu_W^\top(t, X^\varepsilon(t-))dW(t) \quad (3.21)$$

$$dZ^\varepsilon = g(t, X^\varepsilon(t-))Y^\varepsilon(t-)dt + G_w^\top(t, X^\varepsilon(t-))Y^\varepsilon(t-)dw(t) + G_W^\top(t, X^\varepsilon(t-))Y^\varepsilon(t-)dW(t) + Y^\varepsilon(t-) \int_{|z| \geq \varepsilon} G_N(t, X^\varepsilon(t-), z)N(dt, dz) - Y^\varepsilon(t-) \int_{|z| \geq \varepsilon} G_N(t, X^\varepsilon(t-), z)\nu(dz)dt. \quad (3.22)$$

Note that the previous system (3.9)-(3.11) is a special case of the above system when $\mu_w = \mu_W = G_w = G_W = G_N = 0$.

We now show that these auxiliary functions can be chosen in such a way that the variance of $\Gamma_{s,x}^\varepsilon(T)$ becomes zero.

Theorem 2. *If the functions μ_w , μ_W , G_w , G_W , and G_N satisfy*

$$u^\varepsilon(t, x)\mu_w(t, x) + G_w(t, x) = -\sigma^\top(t, x)\nabla u^\varepsilon(t, x), \quad (3.23)$$

$$u^\varepsilon(t, x)\mu_W(t, x) + G_W(t, x) = -\beta_\varepsilon^\top F^\top(t, x)\nabla u^\varepsilon(t, x), \quad (3.24)$$

$$G_N(t, x, z) = u^\varepsilon(t, x) - u^\varepsilon(t, x + F(t, x)z), \quad (3.25)$$

for all $(t, x, z) \in [s, T] \times \mathbb{R}^d \times \mathbb{R}^q$, then

$$\text{Var}[\Gamma_{s,x}^\varepsilon(T)] = 0. \quad (3.26)$$

Moreover,

$$u^\varepsilon(s, x) = \Gamma_{s,x}^\varepsilon(T). \quad (3.27)$$

Proof. Applying Ito's formula to $\Gamma_{s,x}^\varepsilon(t)$, we obtain

$$\begin{aligned} \Gamma_{s,x}^\varepsilon(T) &= u^\varepsilon(s, x) \\ &+ \int_s^T Y^\varepsilon \left[\frac{\partial u^\varepsilon}{\partial t} + \frac{1}{2} \sum_{i,j=1}^d a^{ij} \frac{\partial^2 u^\varepsilon}{\partial x^i \partial x^j} + \langle b, \nabla u^\varepsilon \rangle - \langle F\gamma_\varepsilon, \nabla u^\varepsilon \rangle + cu^\varepsilon + g \right] dt \\ &+ \frac{1}{2} \int_s^T Y^\varepsilon \sum_{i,j=1}^d (FB_\varepsilon F^\top)^{ij} \frac{\partial^2 u^\varepsilon}{\partial x^i \partial x^j} dt + \int_s^T Y^\varepsilon (\nabla^\top u^\varepsilon \sigma + u^\varepsilon \mu_w^\top) dw(t) \\ &+ \int_s^T Y^\varepsilon (\nabla u^\varepsilon \beta_\varepsilon^\top F + u^\varepsilon \mu_W^\top) dW(t) + \int_s^T Y^\varepsilon G_w^\top dw(t) + \int_s^T Y^\varepsilon G_W^\top dW(t) \\ &+ \int_s^T \int_{|z| \geq \varepsilon} Y^\varepsilon [u^\varepsilon(t, X^\varepsilon(t-) + Fz) - u^\varepsilon] N(dt, dz) \\ &+ \int_s^T \int_{|z| \geq \varepsilon} Y^\varepsilon G_N N(dt, dz) - \int_s^T \int_{|z| \geq \varepsilon} Y^\varepsilon G_N \nu(dz) dt. \end{aligned}$$

Since u^ε satisfies the PIDE (3.17)-(3.18), we arrive at

$$\begin{aligned}
\Gamma_{s,x}^\varepsilon(T) &= u^\varepsilon(s, x) \\
&+ \int_s^T \int_{|z| \geq \varepsilon} Y^\varepsilon [u^\varepsilon(t, X^\varepsilon(t-) + Fz) - u^\varepsilon] (N(dt, dz) - \nu(dz)dt) \\
&+ \int_s^T \int_{|z| \geq \varepsilon} Y^\varepsilon G_N (N(dt, dz) - \nu(dz)dt) + \int_s^T Y^\varepsilon (\nabla^\top u^\varepsilon \sigma + G_w^\top + u^\varepsilon \mu_w^\top) dw(t) \\
&+ \int_s^T Y^\varepsilon (\nabla u^{\varepsilon \top} F \beta_\varepsilon + G_W^\top + u^\varepsilon \mu_W^\top) dW(t).
\end{aligned} \tag{3.28}$$

Then, it is not difficult to see that

$$\mathbb{E} \Gamma_{s,x}^\varepsilon(T) = u^\varepsilon(s, x), \tag{3.29}$$

regardless of the choice of the auxiliary functions. Moreover, if the conditions (3.23)-(3.25) are satisfied, the integrands in (3.28) become zero and

$$\text{Var} \Gamma_{s,x}^\varepsilon(T) = 0. \tag{3.30}$$

□

3.1 Numerical algorithm

Theorem 2 can be used in the same way as Theorem 1 was used to motivate Algorithm 1. Theorem 2 shows that via an optimal choice of G_w , G_W , and G_N (here we take $\mu_w = \mu_W = 0$) we can achieve a system of SDEs such that the random variable of interest, Γ^ε , has zero variance. Moreover, no matter the choice of G_w , G_W , or G_N we do not introduce any additional bias into the MC approximation which is clear from (3.29). We propose an algorithm whose objective is to find a good approximation of an optimal choice of the functions G_w , G_W , and G_N and which then uses this approximation to simulate low-variance realisations of Γ^ε .

As before, we parameterize G_w , G_W , and G_N with feed-forward neural networks $G_{w,\theta}$, $G_{W,\theta}$, and $G_{N,\theta}$, respectively. We obtain the neural SDEs

$$\begin{aligned}
dX^\varepsilon &= b(t, X^\varepsilon(t-)) - F(t, X^\varepsilon(t-))\gamma_\varepsilon dt + \sigma(t, X^\varepsilon(t-))dw(t) + F(t, X^\varepsilon(t-))\beta_\varepsilon dW(t) \\
&+ \int_{|z| \geq \varepsilon} F(t, X^\varepsilon(t-))zN(dt, ds),
\end{aligned} \tag{3.31}$$

$$dY^\varepsilon = c(t, X^\varepsilon(t-))Y^\varepsilon(t-)dt, \tag{3.32}$$

$$\begin{aligned}
dZ^\varepsilon &= g(t, X^\varepsilon(t-))Y^\varepsilon(t-)dt + G_{w,\theta}^\top(t, X^\varepsilon(t-))Y^\varepsilon(t-)dw(t) \\
&+ G_{W,\theta}^\top(t, X^\varepsilon(t-))Y^\varepsilon(t-)dW(t) + Y^\varepsilon(t-) \int_{|z| \geq \varepsilon} G_{N,\theta}(t, X^\varepsilon(t-), z)N(dt, dz) \\
&- Y^\varepsilon(t-) \int_{|z| \geq \varepsilon} G_{N,\theta}(t, X^\varepsilon(t-), z)\nu(dz)dt.
\end{aligned} \tag{3.33}$$

Define

$$\Gamma_\theta^\varepsilon = f(X^\varepsilon(T))Y^\varepsilon(T) + Z^\varepsilon(T). \tag{3.34}$$

Letting $V(t) = (X(t)^\top, Y(t), Z(t))^\top$ and $v = (x^\top, 1, 0)^\top$, we consider a numerical scheme of the form

$$\bar{V}_{k+1} = \bar{V}_k + A(t_k, \bar{V}_k, h, \xi_k), \tag{3.35}$$

$$\bar{V}_0 = V(s) = v, \tag{3.36}$$

where a deterministic $h > 0$ is a maximum step size, A is a Borel measurable function, and $(\xi_n)_{n \geq 0}$ are appropriately chosen random variables taking into account randomness coming from the Wiener and Poisson processes. We allow for the case of a restricted jump-adapted numerical scheme as e.g. in [9] when, in particular, the number of time steps is random (see further details in Section 4.2).

Algorithm 2 for the Lévy noise case is analogous to the Brownian motion case (Algorithm 1), except we have more sources of noise.

Algorithm 2: Neural control variate method for Lévy-driven SDEs

Result: MC approximation of the solution to the PIDE (3.1)-(3.2), $\bar{u}(s, x_0)$

Initialise: Number of trials for first-pass M_r , number for trials for second-pass M ,
numerical scheme for first-pass (A_r, h_r) , numerical scheme for second-pass
 (A, h)

for $m \leftarrow 1$ **to** M_r **do**

Initialise: $\bar{X}_0, \bar{Y}_0, \bar{Z}_0 \leftarrow x_0, 1, 0$

Compute: $(t_k, \bar{X}_k, \bar{Y}_k, \bar{Z}_k)_{0 \leq k < N}^m$ and $(\bar{\Gamma})^m$ according to (3.31)-(3.33) with
 $G_w = G_W = G_N = 0$ and the scheme (A_r, h_r)

Store: $(t_k, \bar{X}_k, \bar{Y}_k, \bar{Z}_k)_{0 \leq k < N}^m$ and $(\bar{\Gamma})^m$ and random variables $(\xi_k)_{0 \leq k < N}$

end

Compute: $\theta^* = \arg \min_{\theta \in \Theta} \text{Var}_{M_r} \bar{\Gamma}_\theta$ by SGD using the stored trajectories and random
variables to compute $\bar{\Gamma}_\theta$ with the scheme (A_r, h_r) .

for $m \leftarrow 1$ **to** M **do**

Initialise: $\bar{X}_0, \bar{Y}_0, \bar{Z}_0 \leftarrow x_0, 1, 0$

Compute: $\bar{\Gamma}_{\theta^*, m}$ using (3.31)-(3.33) with $G_{w, \theta^*}, G_{W, \theta^*}, G_{N, \theta^*}$ and the numerical
 scheme (A, h)

Store: Updated sample statistics of $\bar{\Gamma}_{\theta^*}$

end

Return: $\bar{u}(s, x_0) = M^{-1} \sum_{m=1}^M \bar{\Gamma}_{\theta^*, m}$

We note that Remark 1 is also applicable in the case of Algorithm 2

Remark 2. *When implementing Algorithm 2, it is computationally expensive to evaluate the double integrals in (3.33). We found that, in practice, replacing the function $G_{N, \theta} : \mathbb{R}^{d+q+1} \rightarrow \mathbb{R}$ with a linear approximation of $G_{N, \theta}$ in z , $g_{N, \theta} : \mathbb{R}^{d+1} \rightarrow \mathbb{R}^q$ is more efficient. In other words,*

$$G_{N, \theta}(t, x, z) \approx g_{N, \theta}(t, x)^\top z. \quad (3.37)$$

This means that the inner integrals need not be numerically approximated at each time step since the values can be computed in advance (and in many cases will be known analytically). Explicitly, the integral in (3.33) becomes

$$\int_{|z| \geq \varepsilon} G_{N, \theta}(t, x, z) \nu(dz) \approx g_{N, \theta}(t, x)^\top \int_{|z| \geq \varepsilon} z \nu(dz), \quad (3.38)$$

and $\int_{|z| \geq \varepsilon} z \nu(dz)$ does not have to be computed at each time step.

Analogously to the discussion on the relative error in the diffusion case at the end of Section 2, let us consider the error of the trained $G_{w, \theta^*}, G_{W, \theta^*}, G_{N, \theta^*}$ in comparison with the optimal G_w^*, G_W^*, G_N^* satisfying the conditions (3.23)-(3.25). It is not difficult to obtain using (3.28) and

Ito's formula that

$$\begin{aligned} \text{Var}\Gamma_{\theta^*} = E \int_s^T (Y_{s,x_0}^\varepsilon(t))^2 & \left[(\nabla^\top u^\varepsilon \sigma + G_{w,\theta^*}^\top)^2 + (\nabla u^{\varepsilon^\top} F \beta_\varepsilon + G_{W,\theta^*}^\top)^2 \right. \\ & \left. + \int_{|z| \geq \varepsilon} (u^\varepsilon(t, X^\varepsilon(t-) + Fz) - u^\varepsilon + G_{N,\theta^*})^2 \nu(dz) \right] dt. \end{aligned}$$

Then, using (3.23)-(3.25), we get that the standard deviation of Γ_{θ^*} gives the weighted error of Γ_{θ^*} :

$$\begin{aligned} & \sqrt{\text{Var}\Gamma_{\theta^*}} \\ & = \left(E \int_s^T Y_{s,x_0}^2(t) \left[|G_{w,\theta^*} - G_w^*|^2 + |G_{W,\theta^*} - G_W^*|^2 + \int_{|z| \geq \varepsilon} (G_{N,\theta^*} - G_N^*)^2 \nu(dz) \right] dt \right)^{1/2}. \end{aligned}$$

Consequently (analogously to (3.39)), ignoring the error of numerical integration, we can view

$$\text{Err}_{\Gamma_{\theta^*}} = \frac{\sqrt{\text{Var}\Gamma_{\theta^*}}}{\mathbb{E}\Gamma_{\theta^*}} \quad (3.39)$$

as the appropriated relative error of the trained G_{w,θ^*} , G_{W,θ^*} and G_{N,θ^*} .

4 Numerical Experiments

In this section, we provide several numerical examples from computational finance to demonstrate efficiency of Algorithms 1 and 2. We consider the cases of the SDEs driven by Lévy processes with infinite activity, finite activity, and being driven only by Brownian motion.

In the paper's spirit of the 'on-the-fly' variance reduction algorithm, we propose to fix an ANN architecture prior to any knowledge of the particular problem. Of course, better results can be achieved if a particular architecture is chosen and/or tuned for each problem. We propose to use a fully-connected feed forward ANN with ReLU activation (see Appendix A). The number of hidden layers and the size of the hidden layers are chosen via a hyperparameter search detailed in Appendix B and the values selected are shown in Table 1. We also make use of batch normalization before the first layer of the network. For the optimization, we use the Adam algorithm [27] with a fixed learning rate of $\eta = 10^{-3}$. All experiments are performed on an NVidia Tesla V100 GPU.

For each experiment, we compare the neural control variate algorithm with vanilla MC. By vanilla MC, we mean MC without the use of control variates or any other variance reduction techniques. This comparison serves as a convenient benchmark since, as a rule, the additional training run of Algorithm 1/2 must be less computationally expensive than simply increasing the number of simulations of vanilla MC. The implementation is carried out in PyTorch and the code is available at https://github.com/piers-hinds/sde_mc.

Both the MC simulations and the training of the ANNs are done on a GPU. MC is particularly efficient to implement in a GPU-supported scientific computing library like PyTorch since each MC simulation can be carried out independently, i.e. in parallel. The corresponding implementation is at https://github.com/piers-hinds/sde_mc (see the `SdeSolver` class which can solve multiple independent trajectories in parallel).

Jump-adapted schemes pose a unique challenge in order to simulate trajectories in parallel, since each trajectory may have a different number of time steps when a jump-adapted numerical scheme is used. Our solution involves storing the time points corresponding to each trajectory, as well as the trajectory itself. Full details of the implementation can be found at https://github.com/piers-hinds/sde_mc (see the `JumpDiffusionSolver` class).

In each experiment, the network is trained on $M_r = 3 \cdot 10^4$ trajectories for a maximum of 20 epochs before being used to generate trajectories. We propose and use a stopping rule for the

training which is explained in Appendix B; the rule allows for the termination of the training early if it becomes too slow. The training trajectories are chosen to have 5 times larger time-step sizes than the trajectories used in the final MC estimation, i.e. $h_r = 5h$, we refer to this value as the step factor. We use a batch size of 2000 in all experiments. We summarize the network hyperparameters in Table 1. In each experiment, the reported time taken includes training time.

Table 1: Hyperparameters and their chosen values

Hyperparameter	Value
Number of hidden layers	3
Hidden layer size	50
Step factor	5
Training data size	$3 \cdot 10^4$

4.1 Diffusion models

In the first two experiments (Sections 4.1.1 - 4.1.2), we use the explicit Euler scheme (see e.g. [34]), which for a system

$$dX(t) = b(t, X)dt + \sigma(t, X)dW(t), \quad X(s) = x, \quad (4.1)$$

is defined by

$$X_0 = X(s) = x, \quad (4.2)$$

$$X_{k+1} = X_k + b_k h + \sigma_k \Delta_k W, \quad (4.3)$$

where $h > 0$ is a fixed step-size and $\Delta_k W$ are independent Gaussian random variables (or, in the case of many Wiener processes, vectors consisting of independent Gaussian random variables) with zero mean and variance h . The step-size used for each experiment is $h = \frac{T-s}{1000}$. In the experiment of Section 4.1.3 we use a custom numerical scheme from [32].

4.1.1 Geometric Brownian motion

Consider the one-dimensional Black-Scholes model, in which the price $u(t, x)$ of a contingent claim satisfies the Black-Scholes equation

$$\frac{\partial u}{\partial t} + \frac{\sigma^2 x^2}{2} \frac{\partial^2 u}{\partial x^2} + rx \frac{\partial u}{\partial x} - ru = 0 \quad (4.4)$$

with terminal condition

$$u(T, x) = f(x), \quad (4.5)$$

where the short rate $r \in \mathbb{R}$ and the volatility $\sigma > 0$. We consider the case of a call option when $f(x) = (x - K)_+$ for various strikes $K > 0$. The problem (4.4)-(4.5) has the following probabilistic representation:

$$u(s, x) = \mathbb{E} \left[f(X_{s,x}(T)) e^{-r(T-s)} + Z_{s,x}(T) \right], \quad (4.6)$$

where

$$dX(t) = rX(t)dt + \sigma X(t)dW(t), \quad X(s) = x, \quad (4.7)$$

$$dZ(t) = G(t, X(t)) e^{-r(t-s)} dW(t), \quad Z(s) = 0. \quad (4.8)$$

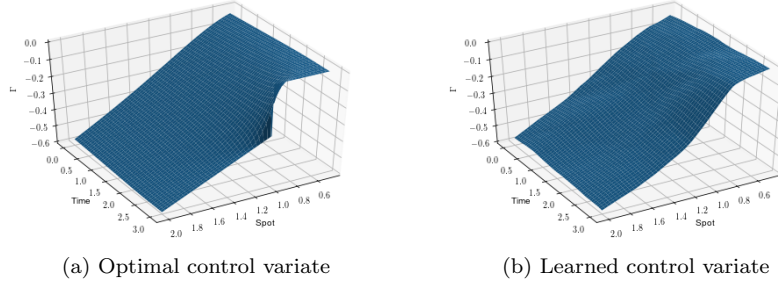


Figure 1: The true optimal control variate and the learned control variate for a European call option with strike $K = 1$ under the Black-Scholes model with parameters in Table 2

Numerical results for various strikes, K , are given in Table 2 for both vanilla MC (i.e. without any control variates) and for our neural variance reduction algorithm. We observe substantial (up to 18 time) speed up of option valuation when the variance reduction is used in comparison with the vanilla MC. The MC tolerance level is set at 10^{-4} in this and all the other experiments, aside from those in Section 4.3 where it is set to 10^{-3} . The relative error given in the table (and in all the other tables of Section 4.1) corresponds to $\text{Err}_{G_{\theta^*}}$ as defined in (2.25).

Figure 1 shows the true optimal control variate, as given by Theorem 1, as well as the learned approximate control variate in the case that $K = 1$. It can be seen that the learned control variate is similar to the optimal control variate but not especially accurate, indicating that high accuracy is not required for the control variate method to be effective.

Table 2: European Call option, $f(x) = (x - K)_+$, under GBM with $r = 0.02$, $\sigma = 0.3$ and $T = 3$: MC approximations (and a 95% confidence interval given after \pm) with and without a control variate.

K	$u(0, 1)$	Vanilla MC			Control Variate MC			Relative Error
		$\hat{u}(0, 1)$	Time (s)	M	$\hat{u}(0, 1)$	Time (s)	M	
0.7	0.39031	0.39043 ± 0.00010	87.2	$1.04 \cdot 10^8$	0.39032 ± 0.00010	5.73	$7.00 \cdot 10^4$	0.034
0.8	0.32826	0.32833 ± 0.00010	80.3	$9.62 \cdot 10^7$	0.32821 ± 0.00010	4.27	$7.00 \cdot 10^4$	0.040
0.9	0.27484	0.27486 ± 0.00010	70.9	$8.49 \cdot 10^7$	0.27478 ± 0.00010	4.31	$7.50 \cdot 10^4$	0.051
1	0.22943	0.22943 ± 0.00010	63.1	$7.56 \cdot 10^7$	0.22940 ± 0.00010	6.17	$1.15 \cdot 10^5$	0.075
1.1	0.19117	0.19115 ± 0.00011	48.4	$5.79 \cdot 10^7$	0.19115 ± 0.00010	6.49	$1.40 \cdot 10^5$	0.098
1.2	0.15914	0.15914 ± 0.00010	46.2	$5.53 \cdot 10^7$	0.15915 ± 0.00010	4.54	$9.00 \cdot 10^4$	0.096
1.3	0.13245	0.13249 ± 0.00010	44.2	$5.29 \cdot 10^7$	0.13247 ± 0.00010	6.48	$1.40 \cdot 10^5$	0.140

4.1.2 Multi-dimensional geometric Brownian motion

Consider now the multi-dimensional Black-Scholes model for dynamics of assets' prices. The price $u(t, x)$ of a contingent claim satisfies the PDE:

$$\frac{\partial u}{\partial t} + \frac{\sigma^2}{2} \sum_{i,j=1}^d \rho^{i,j} x^i x^j \frac{\partial^2 u}{\partial x^i \partial x^j} + r \sum_{i=1}^d x^i \frac{\partial u}{\partial x^i} - ru = 0 \quad (4.9)$$

with terminal condition

$$u(T, x) = f(x), \quad (4.10)$$

where $r \in \mathbb{R}$, $\sigma > 0$ and $(\rho)_{ij} = \rho^{i,j}$ is the correlation matrix of the Brownian motion in the following probabilistic representation:

$$u(s, x) = \mathbb{E} \left[f(X_{s,x}(T)) e^{-r(T-s)} + Z_{s,x}(T) \right], \quad (4.11)$$

and

$$dX^i(t) = rX^i(t)dt + \sigma X^i(t)dW_i(t), \quad X^i(s) = x, \quad i = 1, \dots, d, \quad (4.12)$$

$$dZ(t) = G^\top(t, X(t))e^{-r(t-s)}dW(t), \quad Z(s) = 0, \quad (4.13)$$

$W(t) = (W_1(t), \dots, W_d(t))^\top$, and $W_i(t)$, $i = 1, \dots, d$, are correlated Wiener processes. We consider the case of a call-on-max option, that is an option with the payoff

$$f(x) = (\max(x_1, \dots, x_d) - K)_+. \quad (4.14)$$

Table 3 displays the results for Algorithm 1 in the case $d = 3$ with the parameters $r = 0.02$, $\sigma = 0.3$, $T = 3$, $x = 1$ and the correlation coefficients of the Wiener processes:

$$\rho^{1,2} = 0.7, \quad \rho^{1,3} = 0.2, \quad \rho^{2,3} = -0.3.$$

We again see the benefit of using the control variate method which gives speed up of up to 10 times.

Table 3: Call-on-max rainbow option under three-dimensional GBM with $r = 0.02$, $\sigma = 0.3$, $T = 3$, $x = 1$: Monte Carlo approximations (and a 95% confidence interval) with and without a control variate.

K	$u(0, 1)$	Vanilla MC			Control Variate MC			Relative Error
		$\hat{u}(0, 1)$	Time (s)	M	$\hat{u}(0, 1)$	Time (s)	M	
0.7	-	0.73571 ± 0.00010	187	$1.51 \cdot 10^8$	0.73570 ± 0.00010	20.2	$9.15 \cdot 10^5$	0.066
0.8	-	0.64800 ± 0.00010	188	$1.52 \cdot 10^8$	0.64811 ± 0.00010	20.0	$9.20 \cdot 10^5$	0.076
0.9	-	0.56563 ± 0.00010	185	$1.50 \cdot 10^8$	0.56559 ± 0.00010	20.8	$9.65 \cdot 10^5$	0.088
1	-	0.48988 ± 0.00010	177	$1.44 \cdot 10^8$	0.48984 ± 0.00010	17.5	$7.60 \cdot 10^5$	0.091
1.1	-	0.42146 ± 0.00010	155	$1.26 \cdot 10^8$	0.42150 ± 0.00010	20.2	$9.20 \cdot 10^5$	0.120
1.2	-	0.36085 ± 0.00010	153	$1.24 \cdot 10^8$	0.36098 ± 0.00010	18.8	$8.30 \cdot 10^5$	0.130
1.3	-	0.30781 ± 0.00010	134	$1.08 \cdot 10^8$	0.30784 ± 0.00010	17.1	$7.35 \cdot 10^5$	0.140

4.1.3 Heston Model

Consider the Heston stochastic volatility model [22], under which the price $u(t, x, v)$ of a contingent claim satisfies the PDE:

$$\frac{\partial u}{\partial t} + \frac{1}{2}x^2v \frac{\partial^2 u}{\partial x^2} + \frac{1}{2}\sigma^2v \frac{\partial^2 u}{\partial v^2} + \sigma\rho vx \frac{\partial^2 u}{\partial x \partial v} + rx \frac{\partial u}{\partial x} + \kappa(\theta - v) \frac{\partial u}{\partial v} - ru = 0, \quad (4.15)$$

$$u(T, x, v) = f(x), \quad (4.16)$$

where $\kappa > 0$, $\theta > 0$, $\sigma > 0$, $\rho \in (-1, 1)$ and $r \in \mathbb{R}$, such that $2\kappa\theta > \sigma^2$. The terminal condition, $f(x)$, corresponds to the payoff function. We consider the case of a European call option where

$$f(x) = (x - K)_+, \quad (4.17)$$

for some strike price $K > 0$. The Heston PDE problem (4.15)-(4.16) has a probabilistic representation of the form:

$$u(s, x, v) = \mathbb{E} \left[f(X_{s,x,v}(T)) e^{-r(T-s)} + Z_{s,x,v}(T) \right], \quad (4.18)$$

$$dX(t) = rX(t)dt + \sqrt{V(t)}X(t)dW_1(t), \quad X(s) = x, \quad (4.19)$$

$$dV(t) = \kappa(\theta - V(t)) + \sigma\sqrt{V(t)}\left(\rho dW_1(t) + \sqrt{1-\rho^2}dW_2(t)\right), \quad V(s) = v, \quad (4.20)$$

$$dZ(t) = G(t, X(t), V(t))e^{-r(t-s)}dW(t), \quad Z(s) = 0, \quad (4.21)$$

where $W(t) = (W_1(t), W_2(t))^\top$ is a two-dimensional standard Wiener process.

To simulate trajectories of (4.19)-(4.20), we use the explicit Euler scheme for X and the fully implicit Euler scheme for V [32]. For a step-size $h > 0$,

$$X_{k+1} = X_k + rX_k h + \sqrt{V_k}X_k \Delta_k W, \quad (4.22)$$

$$V_{k+1} = V_k + \kappa(\theta - V_{k+1})h - \frac{\sigma^2}{2}h + \sigma\sqrt{V_{k+1}}\Delta_k W. \quad (4.23)$$

The importance of using the fully implicit Euler scheme for V lies in the fact that the explicit Euler scheme does not necessarily preserve positivity of V , while the semi-implicit scheme (4.22)-(4.23) guarantees positivity of V under $\kappa\theta \geq \sigma^2/2$ [32]. Note that the implicitness in (4.23) can be resolved analytically by solving the quadratic equation. The results are presented in Table 4, which demonstrates efficiency of the proposed control variate method, it is up to 42 time faster than vanilla MC.

Table 4: European Call option under the Heston model with $v = 0.15$, $r = 0.02$, $\kappa = 0.25$, $\theta = 0.5$, $\sigma = 0.3$, $\rho = -0.3$, $T = 3$: MC approximations (and a 95% confidence interval) with and without a control variate.

K	$u(0, 1)$	Vanilla MC			Control Variate MC			Relative Error
		$\hat{u}(0, 1)$	Time (s)	M	$\hat{u}(0, 1)$	Time (s)	M	
0.7	0.47517	0.47520 \pm 0.00010	1360	3.09 \cdot 10 ⁸	0.47519 \pm 0.00008	45.3	2.58 \cdot 10 ⁶	0.14
0.8	0.42623	0.42625 \pm 0.00011	1120	2.57 \cdot 10 ⁸	0.42636 \pm 0.00010	30.9	1.65 \cdot 10 ⁶	0.16
0.9	0.38271	0.38274 \pm 0.00010	1180	2.72 \cdot 10 ⁸	0.38267 \pm 0.00011	32.0	1.73 \cdot 10 ⁶	0.19
1	0.34406	0.34401 \pm 0.00010	1070	2.47 \cdot 10 ⁸	0.34407 \pm 0.00009	54.6	3.17 \cdot 10 ⁶	0.24
1.1	0.30977	0.30977 \pm 0.00010	1170	2.7 \cdot 10 ⁸	0.30971 \pm 0.00010	27.4	1.43 \cdot 10 ⁶	0.20
1.2	0.27934	0.27927 \pm 0.00009	1250	2.88 \cdot 10 ⁸	0.27927 \pm 0.00011	39.5	2.20 \cdot 10 ⁶	0.28
1.3	0.25232	0.25230 \pm 0.00010	990	2.28 \cdot 10 ⁸	0.25232 \pm 0.00010	46.3	2.61 \cdot 10 ⁶	0.34

4.2 Non-singular Lévy measure

In this section and the subsequent section (Section 4.3), we use the restricted jump-adapted numerical integration scheme from [9, Algorithm 1]. Here we give its brief description for completeness.

For the SDEs

$$dX = b(t, X) - F(t, X)\gamma_\epsilon dt + \sigma(t, X)dw(t) + F(t, X)\beta_\epsilon dW(t) + \int_{|z| \geq \epsilon} F(t, X)zN(dt, dz), \quad (4.24)$$

$$X(s) = x, \quad (4.25)$$

we set $X_0 = x$ and obtain the approximation X_{k+1} from X_k as follows. We find the next time-step $\theta = \delta \wedge h$, where $h > 0$ is the pre-defined maximum step-size and δ is the time to the next

jump sampled with the intensity $\lambda_\varepsilon = \int_{|z| \geq \varepsilon} \nu(z)$. Then, if $\theta = h$, we use the standard explicit Euler scheme with no jumps. If $\theta < h$, we use

$$X_{k+1} = X_k + (b_k - F_k)\gamma_\varepsilon\theta + \sigma_k\Delta_k w + F_k\beta_\varepsilon\Delta W_k + F_k J, \quad (4.26)$$

where $\Delta_k w$ and $\Delta_k W$ are the respective Brownian increments over the step θ and J is the size of the jump, sampled (independently of other jumps, δ , $\Delta_k w$ and $\Delta_k W$) according to the density

$$\rho_\varepsilon(z) := \frac{\nu(z)\mathbb{1}_{|z| > \varepsilon}}{\lambda_\varepsilon}. \quad (4.27)$$

The approximations for Y and Z are simulated using the explicit Euler scheme, with the same random time step θ as X . The (maximum) step-size used in all the experiments is $h = \frac{T-s}{1000}$.

4.2.1 Merton model

Consider the one-dimensional Merton jump-diffusion model [30], under which the price $u(t, x)$ of a contingent claim satisfies the PIDE:

$$\begin{aligned} & \frac{\partial u}{\partial t}(t, x) + \frac{1}{2}\sigma^2 x^2 \frac{\partial^2 u}{\partial x^2}(t, x) + (r - \beta\lambda)x \frac{\partial u}{\partial x}(t, x) - ru(t, x) \\ & + \frac{\lambda}{\sqrt{2\pi\gamma^2}} \int_{\mathbb{R}} [u(t, xe^z) - u(t, x)] \exp\left\{-\frac{(z - \alpha^2)}{2\sigma^2}\right\} dz = 0, \end{aligned} \quad (4.28)$$

where $r \in \mathbb{R}$, $\sigma > 0$, $\lambda > 0$, $\alpha, \gamma \in \mathbb{R}$ and $\beta = \exp(\alpha + \frac{1}{2}\gamma^2) - 1$. The terminal condition is given by

$$u(T, x) = f(x). \quad (4.29)$$

The probabilistic representation of (4.28)-(4.29) takes the form:

$$u(s, x) = \mathbb{E}\left[f(X_{s,x}(T))e^{-r(T-s)} + Z_{s,x}(T)\right] \quad (4.30)$$

with

$$dX(t) = X(t-)((r - \lambda\beta)dt + \sigma dW(t) + J(t)dN(t)), \quad X(s) = x, \quad (4.31)$$

$$dZ(t) = G_W(t, X(t))e^{-r(t-s)}dW(t) + G_N(t-, X(t-))e^{-r(t-s)}J(t)dN(t) \quad (4.32)$$

$$- \lambda e^{-r(t-s)} \int_{\mathbb{R}} G_N(t, X)z \exp\left\{-\frac{(z - \alpha^2)}{2\sigma^2}\right\} dz dt, \quad Z(s) = 0.$$

where $W(t)$ is a one-dimensional standard Wiener process and $N(t)$ is a Poisson process with intensity λ . The jumps have a shifted log-normal distribution:

$$J_i = \exp(\eta_i) - 1, \quad i = 1, 2, \dots$$

with $\eta_i \sim \mathcal{N}(\alpha, \gamma^2)$. The mean jump size is $\mathbb{E}J_1 =: \beta = \exp(\alpha + \frac{1}{2}\gamma^2) - 1$. The price of a European call option, $u(t, x)$, has the terminal condition

$$f(x) = (x - K)_+,$$

for a strike price $K > 0$.

Table 5 shows the results of Algorithm 2 in the case of $r = 0.02$, $\sigma = 0.2$, $\lambda = 1$, $\alpha = -0.05$, $\gamma = 0.3$. The proposed control variates method here is up to 30 times faster than vanilla MC. The relative error given in the table (and in all the other tables in the next subsections) corresponds to $\text{Err}_{G_{\theta^*}}$ as defined in (3.39).

Table 5: European Call option under Merton model with $r = 0.02$, $\sigma = 0.2$, $\lambda = 1$, $\alpha = -0.05$, $\gamma = 0.3$ and $T = 3$: MC approximations (and a 95% confidence interval) with and without a control variate.

K	$u(0, 1)$	Vanilla MC			Control Variate MC			Relative Error
		$\hat{u}(0, 1)$	Time (s)	M	$\hat{u}(0, 1)$	Time (s)	M	
0.7	0.41361	0.41346 ± 0.00010	1860	$1.61 \cdot 10^8$	0.41364 ± 0.00010	62.1	$1.40 \cdot 10^6$	0.15
0.8	0.35593	0.35575 ± 0.00009	2010	$1.74 \cdot 10^8$	0.35592 ± 0.00011	85.5	$2.05 \cdot 10^6$	0.21
0.9	0.30592	0.30575 ± 0.00011	1480	$1.28 \cdot 10^8$	0.30604 ± 0.00010	104	$2.49 \cdot 10^6$	0.26
1	0.26298	0.26278 ± 0.00010	1460	$1.27 \cdot 10^8$	0.26302 ± 0.00010	127	$3.09 \cdot 10^6$	0.34
1.1	0.22634	0.22624 ± 0.00011	1200	$1.05 \cdot 10^8$	0.22633 ± 0.00010	140	$3.47 \cdot 10^6$	0.42
1.2	0.19519	0.19502 ± 0.00011	1090	$9.52 \cdot 10^7$	0.19532 ± 0.00010	151	$3.79 \cdot 10^6$	0.51
1.3	0.16877	0.16866 ± 0.00011	949	$8.28 \cdot 10^7$	0.16881 ± 0.00010	167	$4.17 \cdot 10^6$	0.62

4.3 Singular Lévy measure

In this section, we test Algorithm 2 on SDEs driven by Lévy processes with infinite activity of jumps. In this case the algorithm is of particular importance because variance of quantities of interest is typically very large and practical use of such models in financial engineering requires efficient variance reduction.

Consider the process to model an underlier:

$$S_i(t) = S_i(s) \exp \{rt + X_i(t)\}, \quad (4.33)$$

where $r > 0$ and X is a d -dimensional process defined as

$$X(T) = \int_s^T b(t, X(t-))dt + \int_s^T \sigma(t, X(t-))dw(t) + \int_s^T \int_{\mathbb{R}} F(t, X(t-))z\hat{N}(dt, dz), \quad (4.34)$$

with Lévy measure given by

$$\nu(dz) = \begin{cases} C_- e^{-\mu(|z|-1)} dz & \text{if } z < -1, \\ C_- |z|^{-(\alpha+1)} dz & \text{if } -1 \leq z < 0, \\ C_+ |z|^{-(\alpha+1)} dz & \text{if } 0 < z \leq 1, \\ C_+ e^{-\mu(|z|-1)} dz & \text{if } 1 < z, \end{cases} \quad (4.35)$$

where C_- , C_+ and μ are positive constants and $\alpha \in (0, 2)$. Throughout, we take $\sigma(t, x)$ to be a constant matrix, $\sigma(t, x) = \sigma \in \mathbb{R}^{d \times d}$ and $F(t, x) = (f_1, \dots, f_d) \in \mathbb{R}^d$. Since the discounted price processes, $\tilde{S}_i(t) = e^{-rt}S_i(t)$, should be martingales, the drift component $b(t, x)$ is chosen as (see [9] or [1, Sec 5.2])

$$b_i = -\frac{1}{2} \sum_{j=1}^d \sigma_{ij}^2 - \int_{\mathbb{R}} (e^{f_i z} - 1 - f_i z \mathbb{1}_{|z| < 1}) \nu(dz). \quad (4.36)$$

We consider this model in one and four dimensions. In all of the examples, we choose $C_- = C_+ = 1$, $\alpha = 0.5$, $\mu = 2$ and $\varepsilon = 10^{-3}$.

4.3.1 One-dimensional European call

We consider the problem of pricing a European call option under model (4.33)-(4.36) with $d = 1$. Table 6 shows the results for Algorithm 2 in the case of $r = 0.02$, $\sigma_{11} = 0.2$ and $f_1 = 0.2$. The computational speed up achieved here by the proposed control variate method is up to 8 times in comparison with vanilla MC.

Table 6: European Call option under exponential Lévy model (4.33): MC approximations (and a 95% confidence interval) with and without a control variate.

K	$u(0,1)$	Vanilla MC			Control Variate MC			Relative Error
		$\hat{u}(0,1)$	Time (s)	M	$\hat{u}(0,1)$	Time (s)	M	
0.7	-	0.46285±0.00100	225	3.00·10 ⁶	0.46298±0.00095	28.1	1.30000·10 ⁵	0.38
0.8	-	0.41284±0.00101	208	2.79·10 ⁶	0.41376±0.00103	27.8	1.25000·10 ⁵	0.45
0.9	-	0.36926±0.00099	205	2.76·10 ⁶	0.36934±0.00101	25.2	1.40000·10 ⁵	0.52
1	-	0.33181±0.00100	193	2.58·10 ⁶	0.33189±0.00100	29.4	1.35000·10 ⁵	0.57
1.1	-	0.29821±0.00102	175	2.34·10 ⁶	0.29721±0.00098	25.7	1.25000·10 ⁵	0.59
1.2	-	0.26838±0.00102	166	2.22·10 ⁶	0.26841±0.00101	27.3	1.40000·10 ⁵	0.72
1.3	-	0.24385±0.00105	148	1.99·10 ⁶	0.24272±0.00105	25.4	1.45000·10 ⁵	0.84

4.3.2 Four-dimensional call-on-max option

As before, consider the model (4.33)-(4.36) with $d = 4$ and the terminal condition

$$f(x) = (\max(x_1, x_2, x_3, x_4) - K)_+ \quad (4.37)$$

for some $K > 0$. Table 7 shows the results of Algorithm 2 in the case of $r = 0.02$, $f = (0.2, 0.15, 0.15, 0.1)^\top$ and

$$\sigma = 0.15L, \quad (4.38)$$

where L is the lower triangular matrix obtained via the Cholesky decomposition of the correlation matrix

$$LL^\top = \begin{bmatrix} 1 & 0.87 & 0.94 & 0.86 \\ 0.87 & 1 & 0.87 & 0.93 \\ 0.94 & 0.87 & 1 & 0.96 \\ 0.86 & 0.93 & 0.96 & 1 \end{bmatrix}. \quad (4.39)$$

Here the achieved speed up is up to 14 times.

Table 7: Rainbow call-on-max option under four-dimensional exponential Lévy model (4.33): Monte Carlo approximations (and a 95% confidence interval) with and without a control variate.

K	$u(0,1)$	Vanilla MC			Control Variate MC			Relative Error
		$\hat{u}(0,1)$	Time (s)	M	$\hat{u}(0,1)$	Time (s)	M	
0.7	-	0.61422±0.00100	699	2.28·10 ⁶	0.61501±0.00101	47.9	1.00·10 ⁵	0.26
0.8	-	0.53704±0.00099	699	2.28·10 ⁶	0.53739±0.00080	72.9	1.65·10 ⁵	0.31
0.9	-	0.46754±0.00100	650	2.12·10 ⁶	0.46939±0.00103	51.1	1.05·10 ⁵	0.36
1	-	0.40659±0.00100	623	2.03·10 ⁶	0.40621±0.00100	50.3	1.10·10 ⁵	0.42
1.1	-	0.35247±0.00101	574	1.87·10 ⁶	0.35399±0.00098	60.2	1.25·10 ⁵	0.50
1.2	-	0.30811±0.00102	530	1.72·10 ⁶	0.30763±0.00097	56.9	1.25·10 ⁵	0.57
1.3	-	0.26923±0.00099	510	1.68·10 ⁶	0.26925±0.00100	61.6	1.40·10 ⁵	0.71

4.4 Transfer learning

In the previous experiments, we initialise the weights of the ANN each time the parameters of the financial model change. However, if the change in parameters is small, e.g. when we vary the strike price while keeping the other parameters fixed, we can use the previous weights of the ANN as the initial weights of the next ANN. This approach is termed as transfer learning (see e.g. [20]). Such a procedure can reduce computational costs further by decreasing the training time. We demonstrate this with the following example. Consider the same experiment as in

Section 4.1.2 (see Table 3). Table 8 shows the time taken for the control variate method from Table 3, where the weights of the ANN are initialised each time, compared to the method of transfer learning where the weights are only initialised once. Note that there is no difference in time for $K = 0.7$, since the weights are initialised in the same way. We see that using transferred weights can give up to 2 times of further speed up, giving overall speed-up up to 20 times in comparison with the plain vanilla MC. Hence, transfer learning can further accelerate variance reduction offered by Algorithms 1 and 2.

Table 8: Experiment from Section 4.1.2: comparison of times using weights re-initialised and weights transferred from previous simulations with different K .

K	Time using new weights	Time using transferred weights
0.7	20.2	20.2
0.8	20.0	11.5
0.9	20.8	10.2
1	17.5	8.6
1.1	20.2	8.3
1.2	18.8	11.0
1.3	17.1	8.1

5 Conclusions

In this paper we proposed novel Monte Carlo (MC) algorithms based on neural SDEs with control variates parameterized by neural networks, which effectively simulate SDEs with substantially reduced variance via efficient approximation of optimal control variates. We considered both SDEs driven by Wiener processes and by general Lévy processes including those with infinite activity. The use of deep learning allows us to find effective control variates on the fly (i.e., without prior training of a neural network) in a truly black-box fashion, in comparison with the use of linear regression for this purpose, where a careful selection of basis functions are needed separately for each model [33]. In numerical tests, we demonstrated that the proposed neural control variate MC can achieve a speed-up up to 40 times in comparison with the plain vanilla MC. Doing training of the network online is attractive from the practical perspective as it can be used immediately within the MC simulation and we showed in several numerical tests that it is efficient. An alternative to the exploited here online training is to train networks offline, which need to be done for any practical use in a parametric space, including parameters of the model for underliers and the payoff. Such a training procedure is typically computationally very costly and hence this approach requires knowing well in advance which model and its range of parameters are of future potential interest – in contrast to our approach where we train networks on the fly. The natural limitation of our algorithms is the dimension of the system of SDEs. They work well for relatively low dimensional SDEs as those typically used in financial engineering, when the cost of network training for a single set of parameters on a fly is relatively low. For larger systems, say of dimension 10 or more, the use of the neural control variates would normally require pre-training of networks (see e.g., [45]) in a parametric space. As usual (see, e.g., [34, 45]), the considered variance reduction does not introduce an additional bias, which is controlled in the standard fashion by a choice of a numerical method and an integration step [34] and which can be estimated in practice using the Talay-Tubaro expansion [42, 34]. The Monte Carlo error is also estimated in the usual way. In other words, the use of deep learning here (similarly to [45]) does not introduce errors which cannot be estimated theoretically or in

practice. We considered here SDEs in the whole \mathbb{R}^d and we note that the proposed algorithms can be applied together with suitable SDEs' approximations [34] in the case of SDEs in bounded domains in \mathbb{R}^d , e.g. with an absorption condition on the boundary, which can be used for pricing barrier options.

Acknowledgement

We are grateful for access to the University of Nottingham's Augusta HPC service.

Declarations of Interest

The authors report no conflicts of interest. The authors alone are responsible for the content and writing of the paper.

References

- [1] Applebaum, D. *Lévy Processes and Stochastic Calculus*. 2nd ed. Cambridge: Cambridge University Press, 2009.
- [2] Asmussen, S. and Rosiński, J. "Approximations of small jumps of Lévy processes with a view towards simulation". *J. Appl. Probab.* 38(2) (2001), pp. 482–493.
- [3] Barron, A. R. "Approximation and estimation bounds for artificial neural networks". *Machine Learning* 14(1) (1994), pp. 115–133.
- [4] Belomestny, D., Häfner, S., Nagapetyan, T., and Urusov, M. "Variance reduction for discretised diffusions via regression". *J. Mathem. Anal. Applic.* 458(1) (2018), pp. 393–418.
- [5] Berner, J., Grohs, P., Kutyniok, G., and Petersen, P. "The modern mathematics of deep learning". *arXiv:2105.04026* (2021).
- [6] Brigo, D. and Mercurio, F. *Interest rate models – theory and practice: with smile, inflation and credit*. Berlin: Springer, 2006.
- [7] Cont, R. and Tankov, P. *Financial modelling with jump processes*. Boca Raton: Chapman & Hall/CRC, 2004.
- [8] Cybenko, G. "Approximation by superpositions of a sigmoidal function". *Mathematics of Control, Signals, and Systems* 2(4) (1989), pp. 303–314.
- [9] Deligiannidis, G., Maurer, S., and Tretyakov, M. V. "Random walk algorithm for the Dirichlet problem for parabolic integro-differential equation". *BIT Numer. Math.* 61(4) (2021), pp. 1223–1269.
- [10] Dick, J., Kuo, F., and Sloan, I. "High-dimensional integration: the quasi-Monte Carlo way". *Acta Numerica* 22 (2013), pp. 133–288.
- [11] Dingerç, K. D. and Hörmann, W. "A general control variate method for option pricing under Lévy processes". *European J. Oper. Research* 221(2) (2012), pp. 368–377.
- [12] Dynkin, E. B. *Markov processes*. Berlin: Springer, 1965.
- [13] Freidlin, M. I. *Functional integration and partial differential equations*. Princeton: Princeton Univ. Press, 1985.
- [14] Friedman, A. *Stochastic differential equations and applications*. Berlin: Springer, 2011.
- [15] Garroni, M. G. and Menaldi, J. L. *Second order elliptic integro-differential problems*. New York: Chapman & Hall/CRC, 2002.

- [16] Geist, M., Petersen, P., Raslan, M., Schneider, R., and Kutyniok, G. “Numerical solution of the parametric diffusion equation by deep neural networks”. *J. Scien. Comp.* 88 (2021).
- [17] Giles, M. B. “Multilevel Monte Carlo methods”. *Acta Numerica* 24 (2015), pp. 259–328.
- [18] Gladyshev, S. A. and Milstein, G. N. “The Runge–Kutta method for calculation of Wiener integrals of functionals of exponential type”. *Zh. Vychisl. Mat. i Mat. Fiz.* 24 (1984), pp. 1136–1149.
- [19] Glasserman, P. *Monte Carlo methods in financial engineering*. Berlin: Springer, 2003.
- [20] Goodfellow, I., Bengio, Y., and Courville, A. *Deep learning*. MIT press, 2016.
- [21] Han, J., Jentzen, A., and E, W. “Solving high-dimensional partial differential equations using deep learning”. *Proc. National Acad. Sci.* 115(34) (2018), pp. 8505–8510.
- [22] Heston, S. L. “A closed-form solution for options with stochastic volatility with applications to bond and currency options”. *Review Finan. Studies* 6 (1993), pp. 327–343.
- [23] Hodgkinson, L., Heide, C. van der, Roosta, F., and Mahoney, M. W. “Stochastic normalizing flows”. *arXiv:2002.09547* (2020).
- [24] Hornik, K., Stinchcombe, M., and White, H. “Multilayer feedforward networks are universal approximators”. *Neural Networks* 2(5) (1989), pp. 359–366.
- [25] Kampen, N. G. van. *Stochastic processes in physics and chemistry*. 3rd ed. Amsterdam: North Holland, 2007.
- [26] Kidger, P., Foster, J., Li, X., and Lyons, T. J. “Neural SDEs as infinite-dimensional GANs”. *Intern. Confer. Machine Learning*. Vol. 139. PMLR, 2021, pp. 5453–5463.
- [27] Kingma, D. P. and Ba, J. “Adam: a method for stochastic optimization”. *Intern. Confer. Learning Representations* (2015).
- [28] Kohatsu-Higa, A., Ortiz-Latorre, S., and Tankov, P. “Optimal simulation schemes for Lévy driven stochastic differential equations”. *Math. Comp.* 83 (2014), pp. 2293–2324.
- [29] Kyprianou, A. E. *Introductory lectures on fluctuations of Lévy processes with applications*. Springer, 2006.
- [30] Merton, R. C. “Option pricing when underlying stock returns are discontinuous”. *J. Finan. Econom.* 3(1) (1976), pp. 125–144.
- [31] Milstein, G. N. and Schoenmakers, J. G. M. “Monte Carlo construction of hedging strategies against multi-asset European claims”. *Stoch. Stoch. Reports* 73(1-2) (2002), pp. 125–157.
- [32] Milstein, G. N. and Tretyakov, M. V. “Numerical analysis of Monte Carlo evaluation of Greeks by finite differences”. *J. Comp. Finance* 8 (2005), pp. 1–33.
- [33] Milstein, G. N. and Tretyakov, M. V. “Practical variance reduction via regression for simulating diffusions”. *SIAM J. Numer. Anal.* 47(2) (2009), pp. 887–910.
- [34] Milstein, G. N. and Tretyakov, M. V. *Stochastic numerics for mathematical physics*. 2nd Edition. Berlin: Springer, 2021.
- [35] Newton, N. J. “Continuous-time Monte Carlo methods and variance reduction”. *Numerical methods in finance*. Ed. by Rogers, L. and Talay, D. Cambridge: Cambridge University Press, 1997, pp. 22–42.
- [36] Newton, N. J. “Variance reduction for simulated diffusions”. *SIAM J. Appl. Math.* 54(6) (1994), pp. 1780–1805.
- [37] Platen, E. and Bruti-Liberati, N. *Numerical solution of stochastic differential equations with jumps in finance*. Berlin: Springer, 2010.

- [38] Shiraya, K. and Takahashi, A. “A general control variate method for multi-dimensional SDEs: An application to multi-asset options under local stochastic volatility with jumps models in finance”. *European J. Oper. Res.* 258(1) (2017), pp. 358–371.
- [39] Shiraya, K., Uenishi, H., and Yamazaki, A. “A general control variate method for Lévy models in finance”. *European J. Oper. Res.* 284(3) (2020), pp. 1190–1200.
- [40] Sirignano, J. and Spiliopoulos, K. “DGM: A deep learning algorithm for solving partial differential equations”. *J. Comput. Phys.* 375 (2018), pp. 1339–1364.
- [41] Su, H., Tretyakov, M. V., and Newton, D. P. “Option valuation through deep learning of transition probability density”. *arxiv:2105.10467* (2021).
- [42] Talay, D. and Tubaro, L. “Expansion of the global error for numerical schemes solving stochastic differential equations”. *Stoch. Anal. Appl.* 8 (1990), pp. 483–509.
- [43] Tretyakov, M. V. *Introductory course on financial mathematics*. London: ICP, 2013.
- [44] Tzen, B. and Raginsky, M. “Neural stochastic differential equations: deep latent Gaussian models in the diffusion limit”. *arXiv:1905.09883* (2019).
- [45] Vidales, M. S., Siska, D., and Szpruch, L. “Unbiased deep solvers for linear parametric PDEs”. *Applied Mathematical Finance* 28(4) (2021), pp. 299–329.
- [46] Wagner, W. “Monte Carlo evaluation of functionals of solutions of stochastic differential equations. Variance reduction and numerical examples”. *Stoch. Anal. Appl.* 6 (1988), pp. 447–468.

Appendix A Artificial Neural Networks

We follow the notation in [5]. For $L \in \mathbb{N}$, $N = (N_0, \dots, N_L) \in \mathbb{N}^{L+1}$ and a Lipschitz function $\rho : \mathbb{R} \rightarrow \mathbb{R}$, a fully connected feed-forward neural network is defined by its architecture $a = (N, \rho)$ and its realization $\Phi_a : \mathbb{R}^{N_0} \times \mathbb{R}^{P(N)} \rightarrow \mathbb{R}^{N_L}$, where $P(N)$ is the number of parameters

$$P(N) := \sum_{l=1}^L N_l N_{l-1} + N_l. \quad (\text{A.1})$$

The realization of the neural network architecture is of the form

$$\Phi_{a,\theta}(x) = W^{(L)} \left(\dots A^{(2)} \left(W^{(2)} \left(A^{(1)} \left(W^{(1)} x + b^{(1)} \right) \right) + b^{(2)} \right) \dots \right) + b^{(L)}, \quad (\text{A.2})$$

where

$$W^{(l)} \in \mathbb{R}^{N_l \times N_{l-1}}, \quad b^{(l)} \in \mathbb{R}^{N_l}, \quad l = 1, \dots, L, \quad (\text{A.3})$$

and $A^{(l)} : \mathbb{R}^{N_l} \rightarrow \mathbb{R}^{N_l}$ is defined by

$$A^{(l)}(x) = \left(\rho(x_1), \dots, \rho(x_{N_l}) \right)^\top, \quad l = 1, \dots, L-1, \quad (\text{A.4})$$

and $\theta = ((W^{(l)}, b^{(l)}))_{l=1}^L \in \mathbb{R}^{P(N)}$. The neural network is said to have $(L-1)$ hidden layers. For further details, see e.g. [20].

Appendix B Discussion of deep learning setup

In this appendix, we provide details concerning hyperparameter estimation and a stopping rule to terminate the training procedure used in the experiments of Section 4.

Fix some tolerance level, $\epsilon > 0$. For the $(1 - \alpha) \times 100\%$ confidence interval of the MC error, let $\mathcal{C} = \mathcal{C}(\epsilon, \alpha)$ denote the total cost of the control variate method (i.e., Algorithm 1/2) required to reach this tolerance level. The total cost \mathcal{C} has two parts: the cost of training $\mathcal{C}_{\text{train}}$ and the cost of running M independent trajectories to compute the quantity of interest $\mathbb{E}\Gamma$. The MC tolerance is equal to

$$\epsilon = \Phi^{-1}(1 - \alpha/2) \frac{\sqrt{\text{Var}\bar{\Gamma}_{\theta^*}}}{\sqrt{M}},$$

and the cost to achieve the corresponding MC simulation is M multiplied by the cost to run a single trajectory. Then, the total cost \mathcal{C} can be conveniently expressed as

$$\mathcal{C} = \mathcal{C}_{\text{train}} + \Phi^{-1}(1 - \alpha/2)^2 \mathcal{C}_{\text{batch}} \frac{\text{Var}\bar{\Gamma}_{\theta^*}}{\epsilon^2 S_{\text{batch}}}, \quad (\text{B.1})$$

where $\mathcal{C}_{\text{batch}}$ is the cost to sample one batch and S_{batch} is the size of the batch (note that the cost of simulating a single trajectory is equivalent to $\mathcal{C}_{\text{batch}}/S_{\text{batch}}$).

B.1 Hyperparameter estimation

In order to choose hyperparameters, i.e. the size of hidden layers, size of training sample, etc., we require a method of evaluating the effectiveness of the variance reduction. Naturally, we would like to choose hyperparameters to minimize the cost \mathcal{C} .

We identify the following hyperparameters: the number of hidden layers in each neural network and the size of these hidden layers (see Appendix A); the reduction factor of the number of steps in the training data compared to the number of steps in the final simulations, which we call the step factor; and the size of the training data. We list each hyperparameter and its corresponding search space in Table 9.

Table 9: Hyperparameters and their possible values.

Hyperparameter	Search space
Number of hidden layers	$\{2, 3, 4\}$
Hidden layer size	$\{20, 30, 40, 50, 60, 70\}$
Step factor	$\{5, 10, 15, 20, 25, 30\}$
Training data size	$\{10^4, 2 \cdot 10^4, 3 \cdot 10^4, 4 \cdot 10^4, 5 \cdot 10^4, 6 \cdot 10^4\}$

In order to determine suitable values of the hyperparameters we minimize the cost \mathcal{C} (with $\alpha = 0.05$, $\epsilon = 10^{-3}$) averaged over four test examples from Section 4. Specifically, we use the experiments from Tables 2, 4, 5 and 6. We employ a grid search over the search space. The optimal values are those given in Table 1 and they are used in the experiments of Section 4.

B.2 Stopping rule for training

Rather than train for a fixed number of epochs for each problem, we propose a stopping rule which will determine when to stop training. On a heuristic level, we want to terminate the training procedure if the cost of training for a further epoch outweighs the variance reduction caused by this further training.

Denote the cost of training for one epoch (we assume that this is consistent across epochs) by $\mathcal{C}_{\text{train}}^{(1)}$. Let $\text{Var}\bar{\Gamma}_{\theta_i}$ denote the reduced variance after the i -th epoch with $\text{Var}\bar{\Gamma}_{\theta_0} := \text{Var}\bar{\Gamma}$. Then, before the i -th epoch, we should decide to stop the training algorithm when

$$\mathcal{C}_{\text{train}}^{(1)} + \Phi^{-1}(1 - \alpha/2)^2 \mathcal{C}_{\text{batch}} \frac{\text{Var}\bar{\Gamma}_{\theta_i}}{\epsilon^2 S_{\text{batch}}} > \Phi^{-1}(1 - \alpha/2)^2 \mathcal{C}_{\text{batch}} \frac{\text{Var}\bar{\Gamma}_{\theta_{i-1}}}{\epsilon^2 S_{\text{batch}}}, \quad (\text{B.2})$$

which is equivalent to

$$\text{Var}\bar{\Gamma}_{\theta_{i-1}} - \text{Var}\bar{\Gamma}_{\theta_i} < \frac{\mathcal{C}_{\text{train}}^{(1)}}{K}, \quad (\text{B.3})$$

where

$$K = \frac{\Phi^{-1}(1 - \alpha/2)^2 \mathcal{C}_{\text{batch}}}{\varepsilon^2 S_{\text{batch}}}. \quad (\text{B.4})$$

Of course, the variance after the i -th epoch is unknown until after the epoch, so we estimate the change $\text{Var}\bar{\Gamma}_{\theta_{i-1}} - \text{Var}\bar{\Gamma}_{\theta_i}$ with the change from the previous epoch, that is $\text{Var}\bar{\Gamma}_{\theta_{i-2}} - \text{Var}\bar{\Gamma}_{\theta_{i-1}}$.

In practice, the cost to train for one epoch, $\mathcal{C}_{\text{train}}^{(1)}$, is estimated during training as the running average of the time taken for one epoch of training. The cost to sample one batch, $\mathcal{C}_{\text{batch}}$, is computed before training takes place.